Electronic Supplementary Material (ESI) for New Journal of Chemistry.

Supporting Information for

Amplification of Impurity upon Complex Formation: How a 2% Ligand Impurity Lowers the Corresponding Complex Purity to 50%

Vageesha W. Liyana Gunawardana and Gellert Mezei*

Department of Chemistry, Western Michigan University, Kalamazoo, Michigan, USA

*Email: gellert.mezei@wmich.edu

CONTENTS **PAGE**

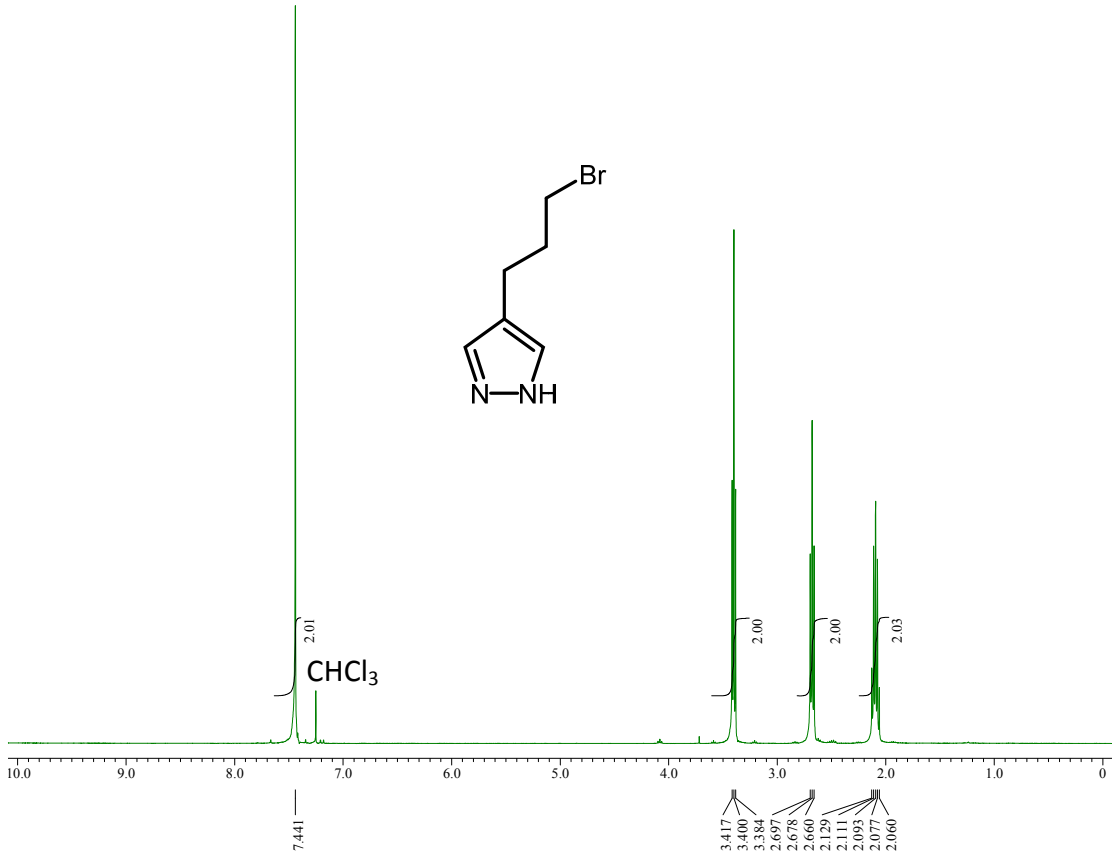

Figure S1. ^{1}H NMR spectrum of **2** in $CDCl_3$.

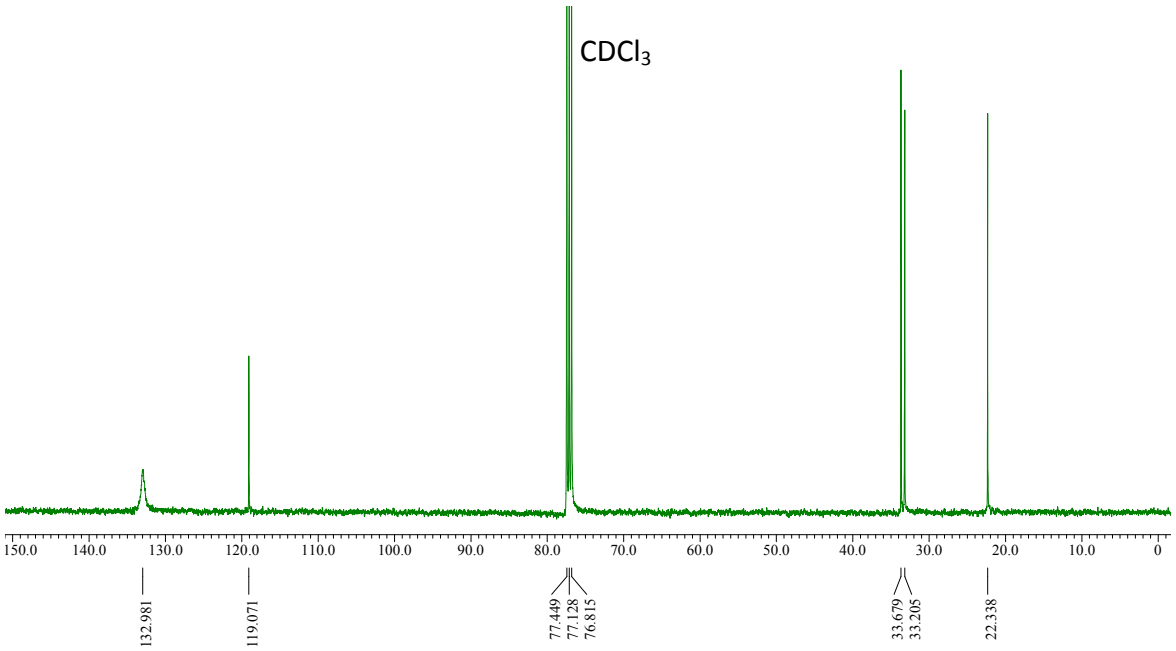

Figure S2. ^{13}C NMR spectrum of **2** in $CDCl_3$.

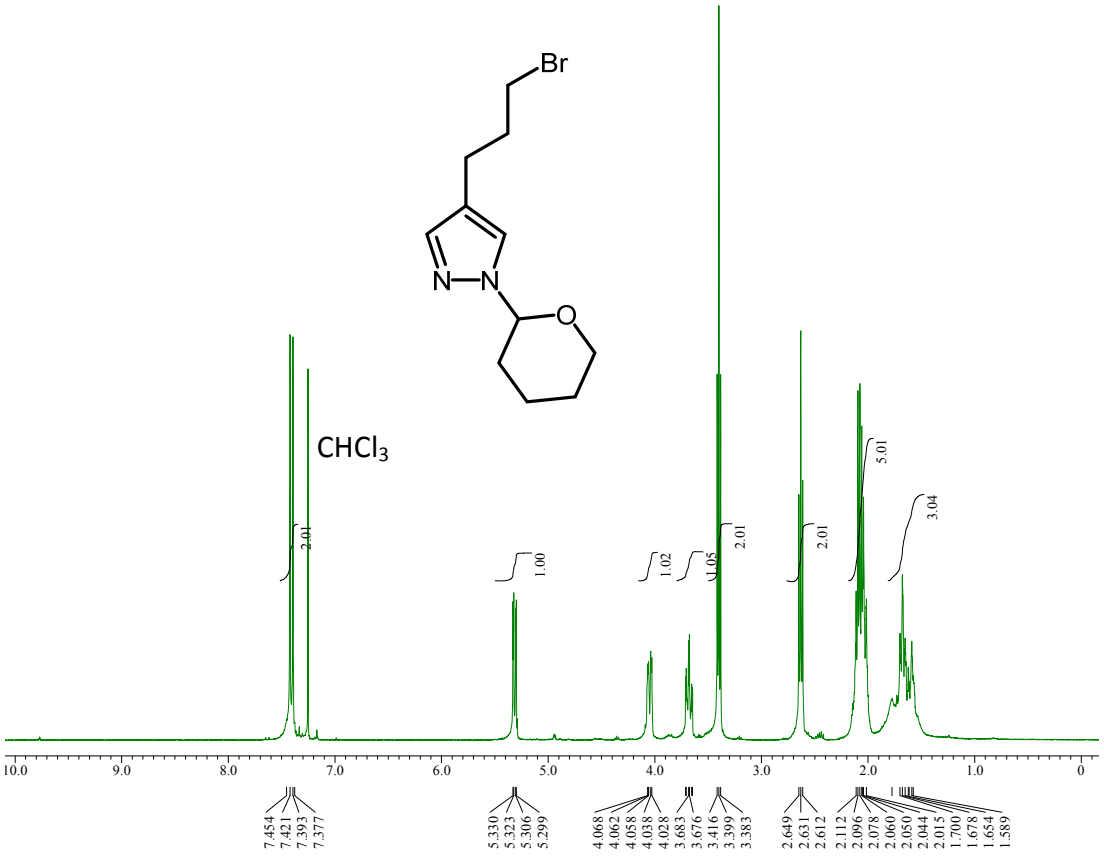

Figure S3. ^{1}H NMR spectrum of **3** in $CDCl_3$.

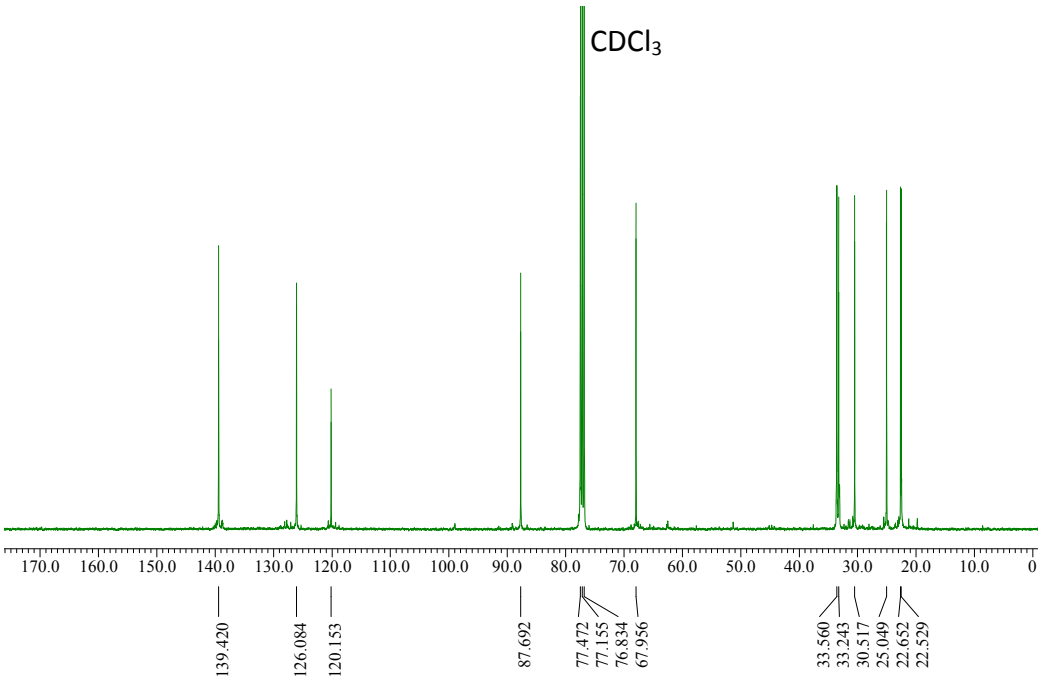

Figure S4. ^{13}C NMR spectrum of **3** in $CDCl_3$.

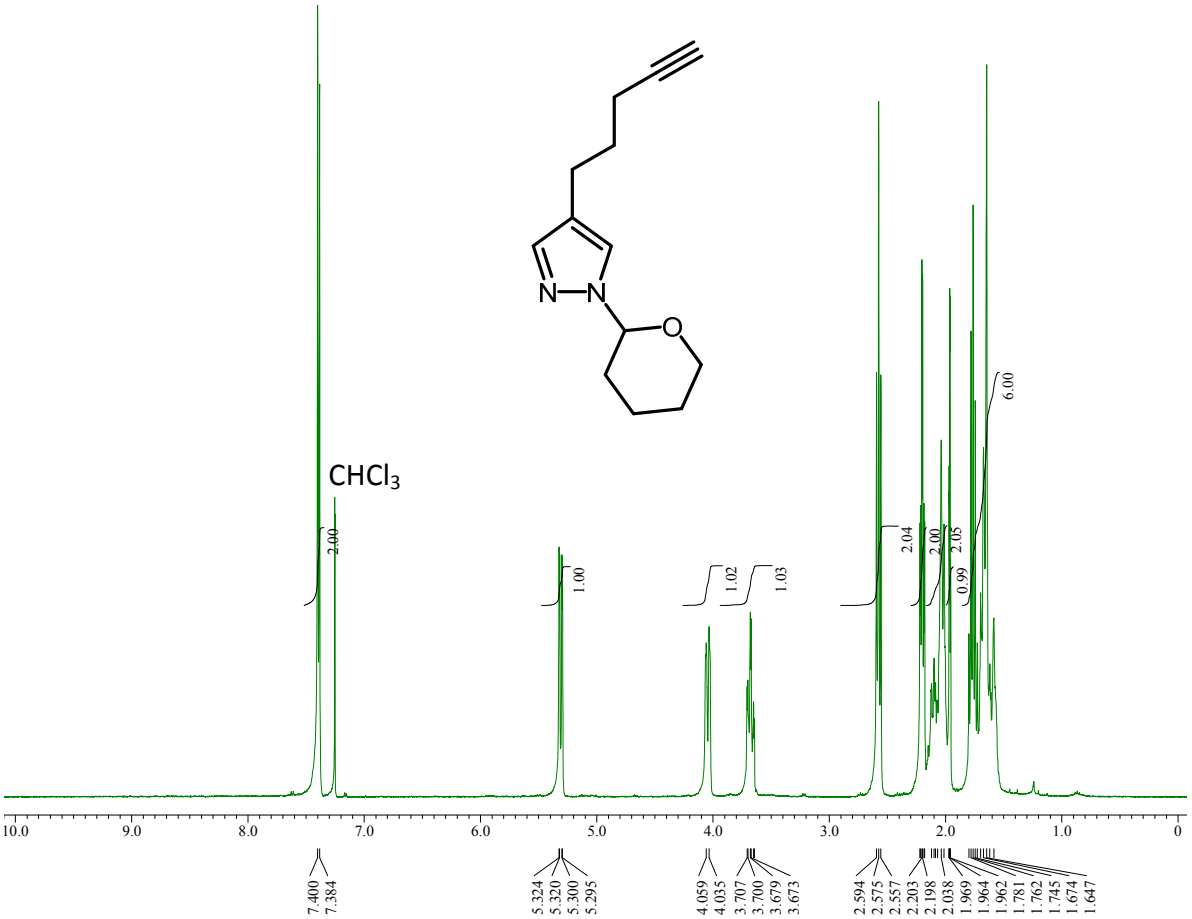

Figure S5. ^{1}H NMR spectrum of **4** in $CDCl_3$.

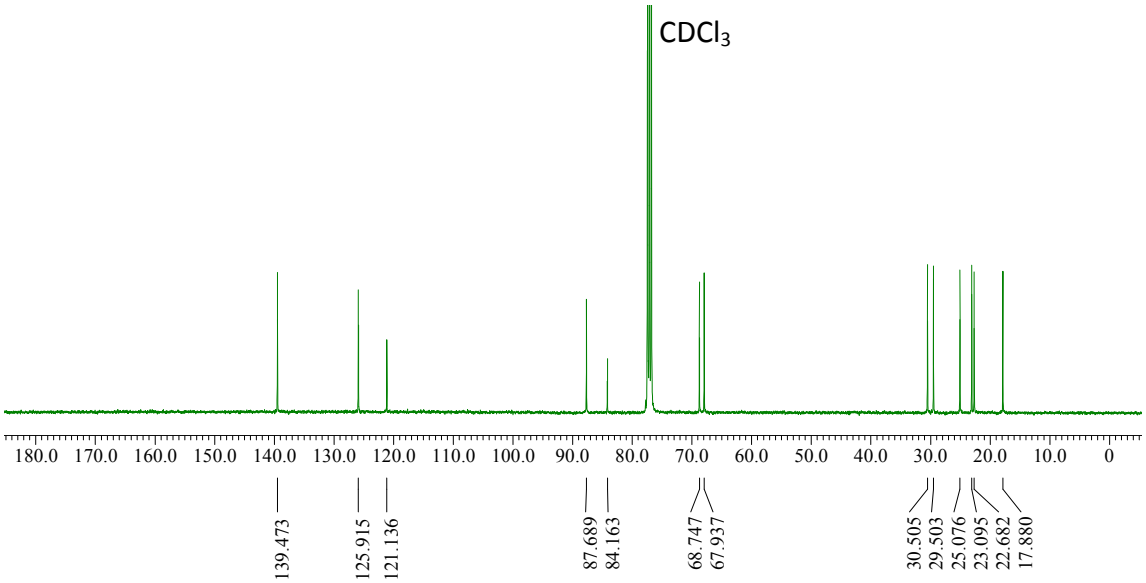

Figure S6. ^{13}C NMR spectrum of **4** in $CDCl_3$.

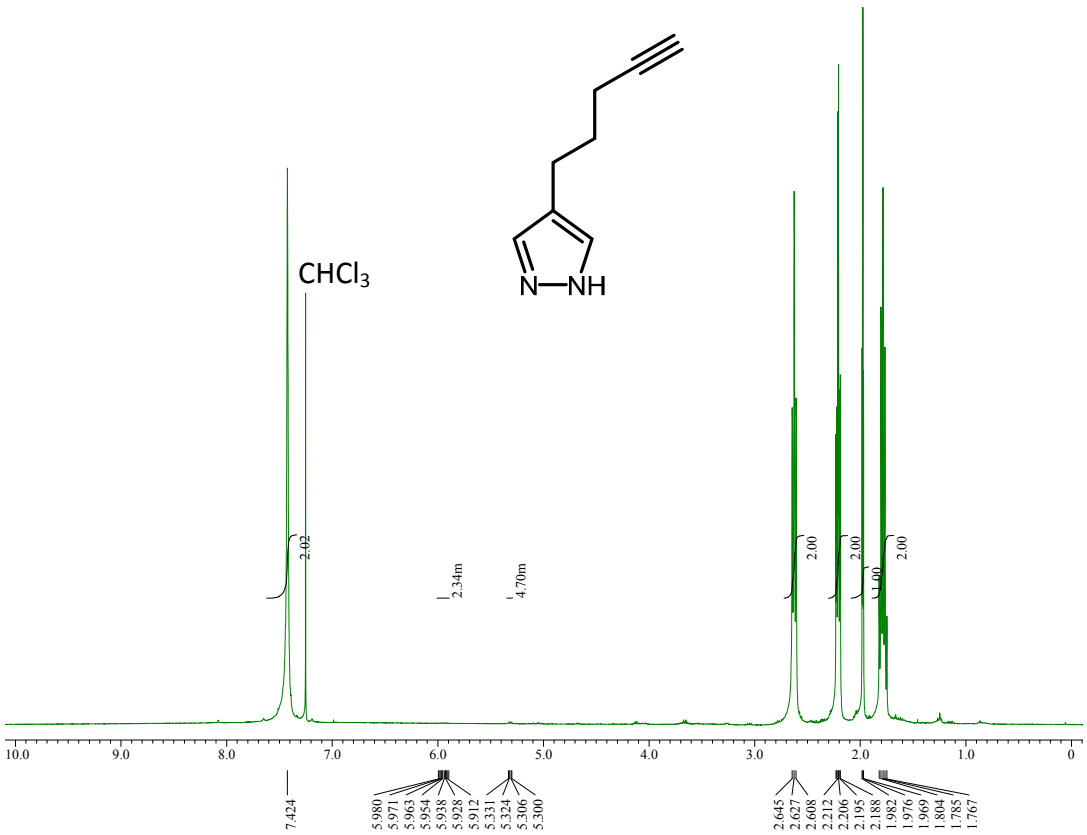

Figure S7. ^{1}H NMR spectrum of **5** in $CDCl_3$.

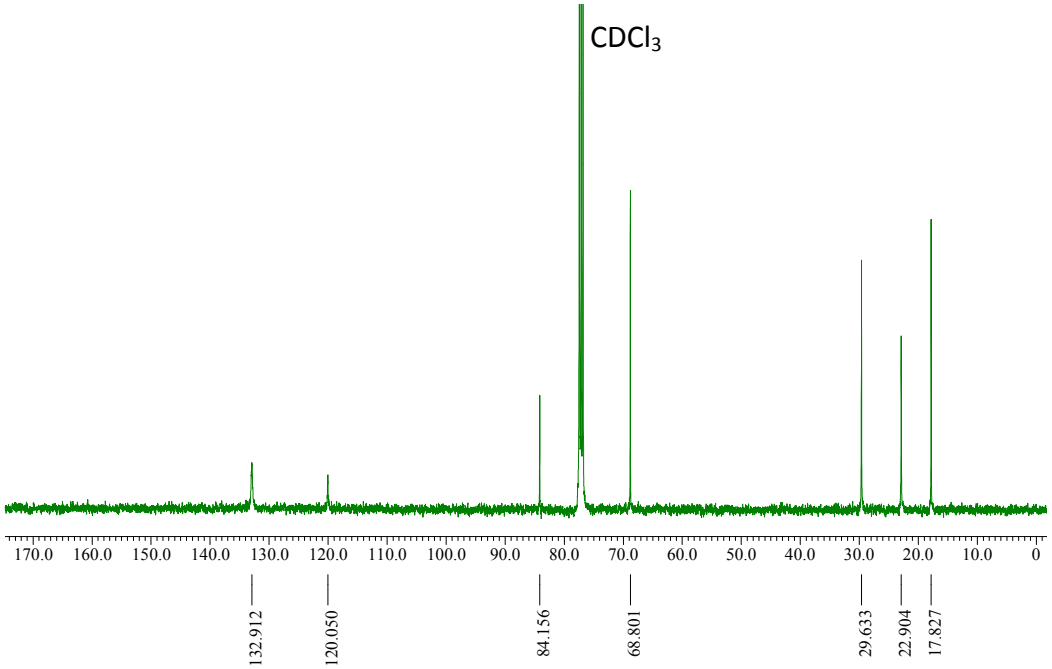

Figure S8. ^{13}C NMR spectrum of **5** in $CDCl_3$.

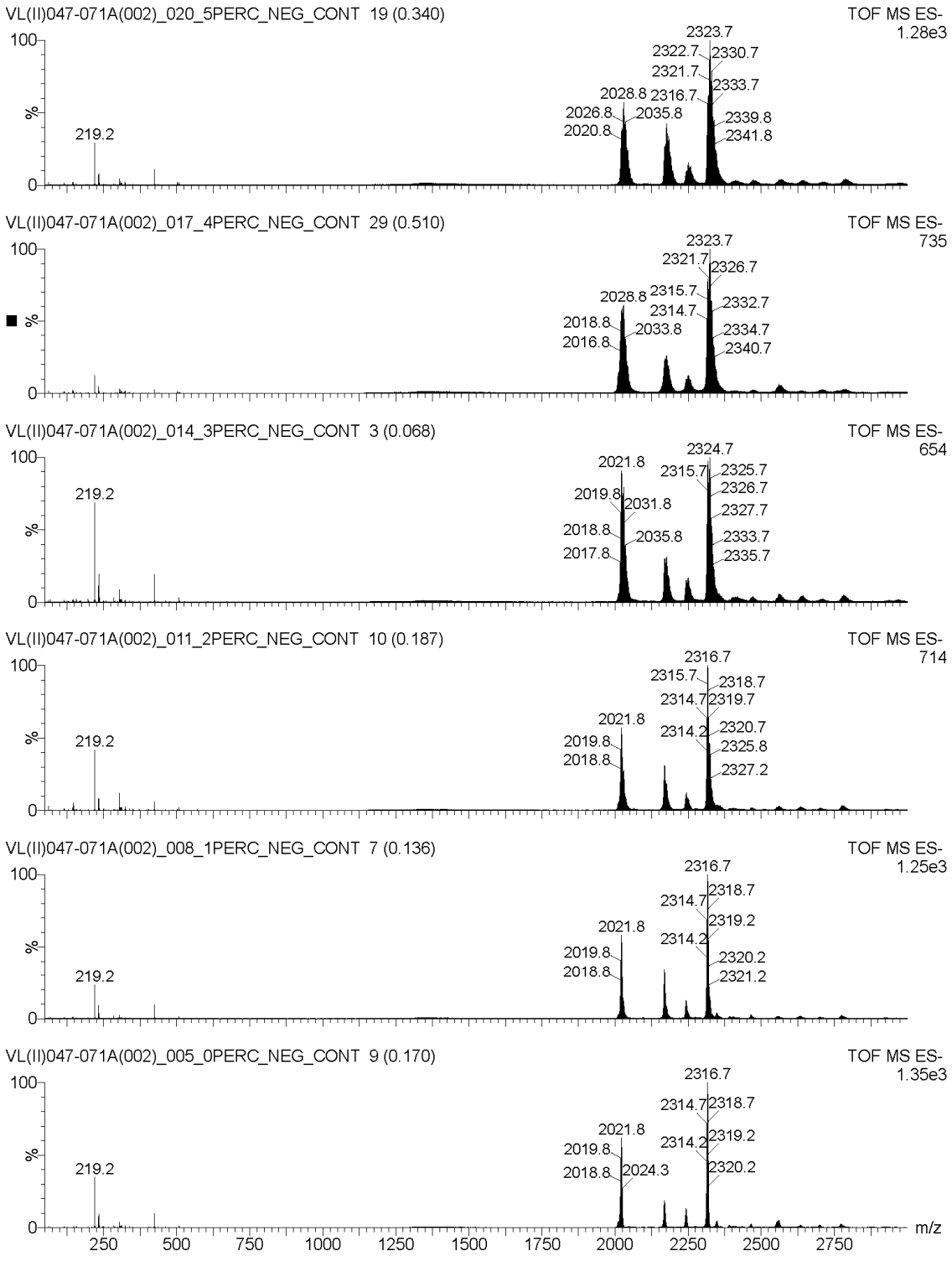

Figure S9. ESI-MS(−) spectra of the $(Bu_4N)_2[CO_3{\subset}\{Cu_n(OH)_n(pz)_{n-x}(4\text{-Mepz})_x\}]$ (n = 27, 29, 30, 31) nanojar mixtures obtained using 0–5 mol% 4-MepzH.

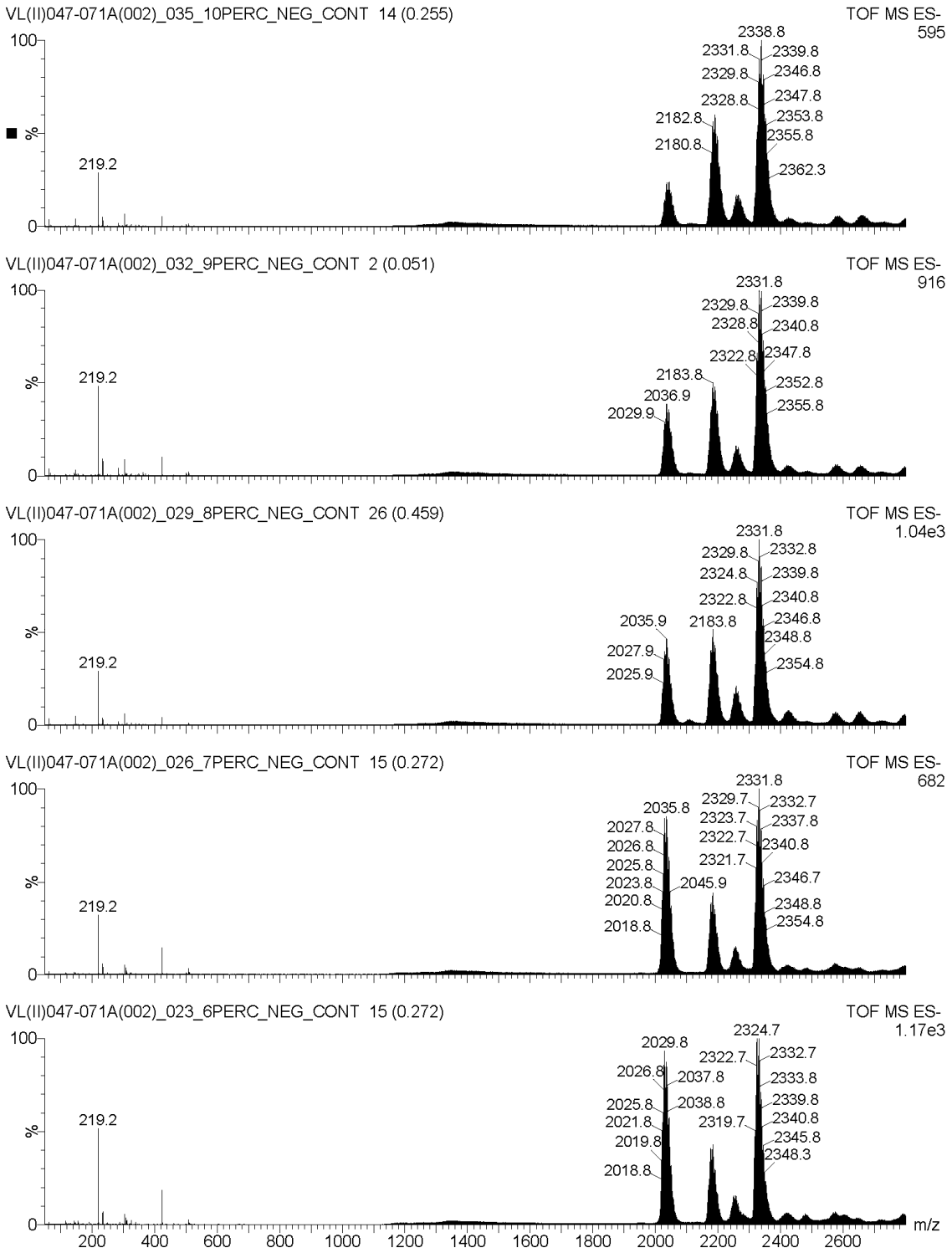

Figure S10. ESI-MS(−) spectra of the $(Bu_4N)_2[CO_3\subset\{Cu_n(OH)_n(pz)_{n-x}(4\text{-Mepz})_x\}]$ (n = 27, 29, 30, 31) nanojar mixtures obtained using 6−10 mol% 4-MepzH.

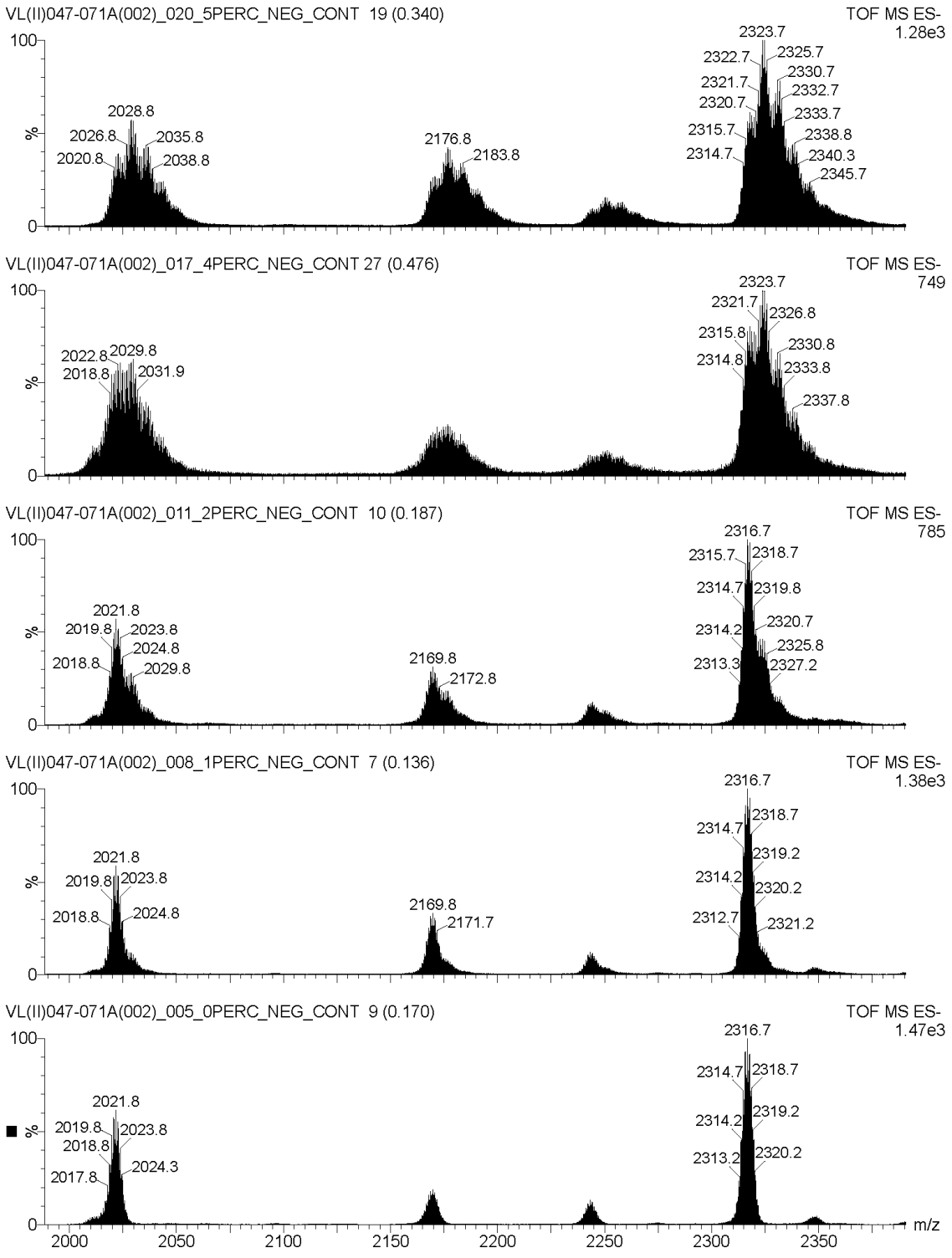

Figure S11. Zoomed portion of the ESI-MS(−) spectra of the $(Bu_4N)_2[CO_3\subset\{Cu_n(OH)_n(pz)_{n-x}(4\text{-Mepz})_x\}]$ (n = 27, 29, 30, 31) nanojar mixtures obtained using 0−5 mol% 4-MepzH.

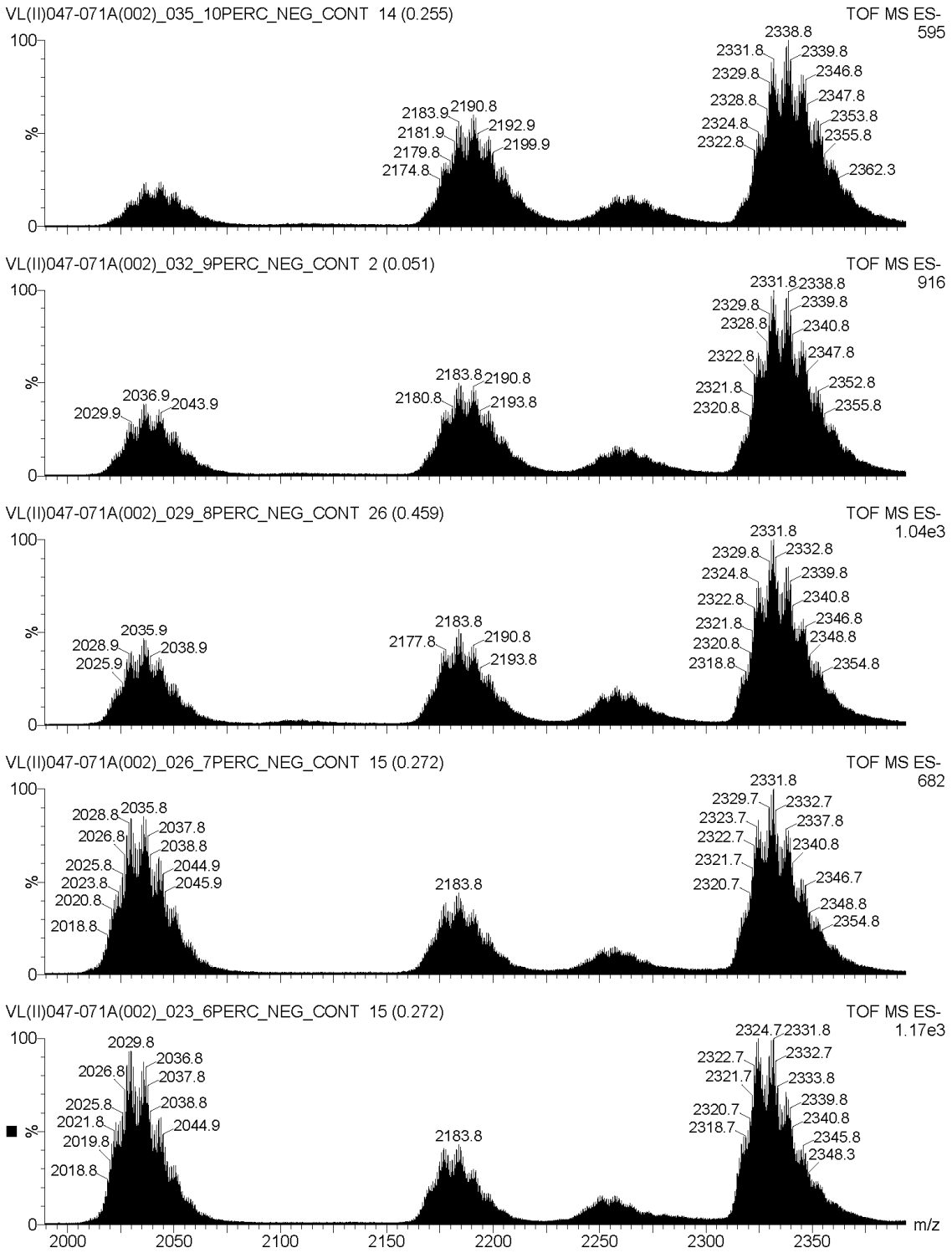

Figure S12. Zoomed portion of the ESI-MS(−) spectra of the $(Bu_4N)_2[CO_3\subset\{Cu_n(OH)_n(pz)_{n-x}(4\text{-Mepz})_x\}]$ (n = 27, 29, 30, 31) nanojar mixtures obtained using 6–10 mol% 4-MepzH.

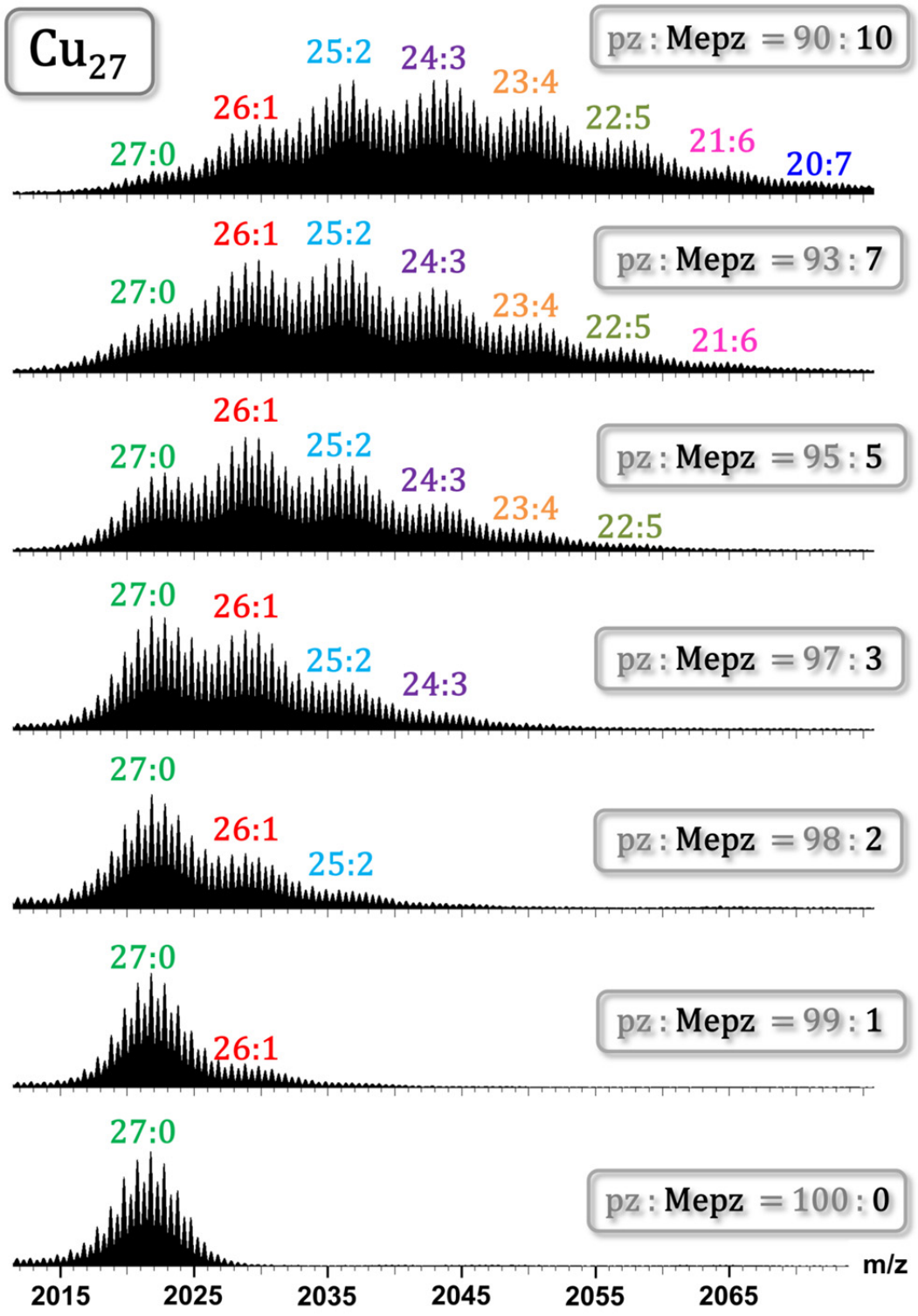

Figure S13. Zoomed portion of the ESI-MS(−) spectra of the $(Bu_4N)_2[CO_3\subset\{Cu_n(OH)_n(pz)_{n-x}(4\text{-Mepz})_x\}]$ (n = 27, 29, 30, 31) nanojar mixtures obtained using 0–10 mol% 4-MepzH.

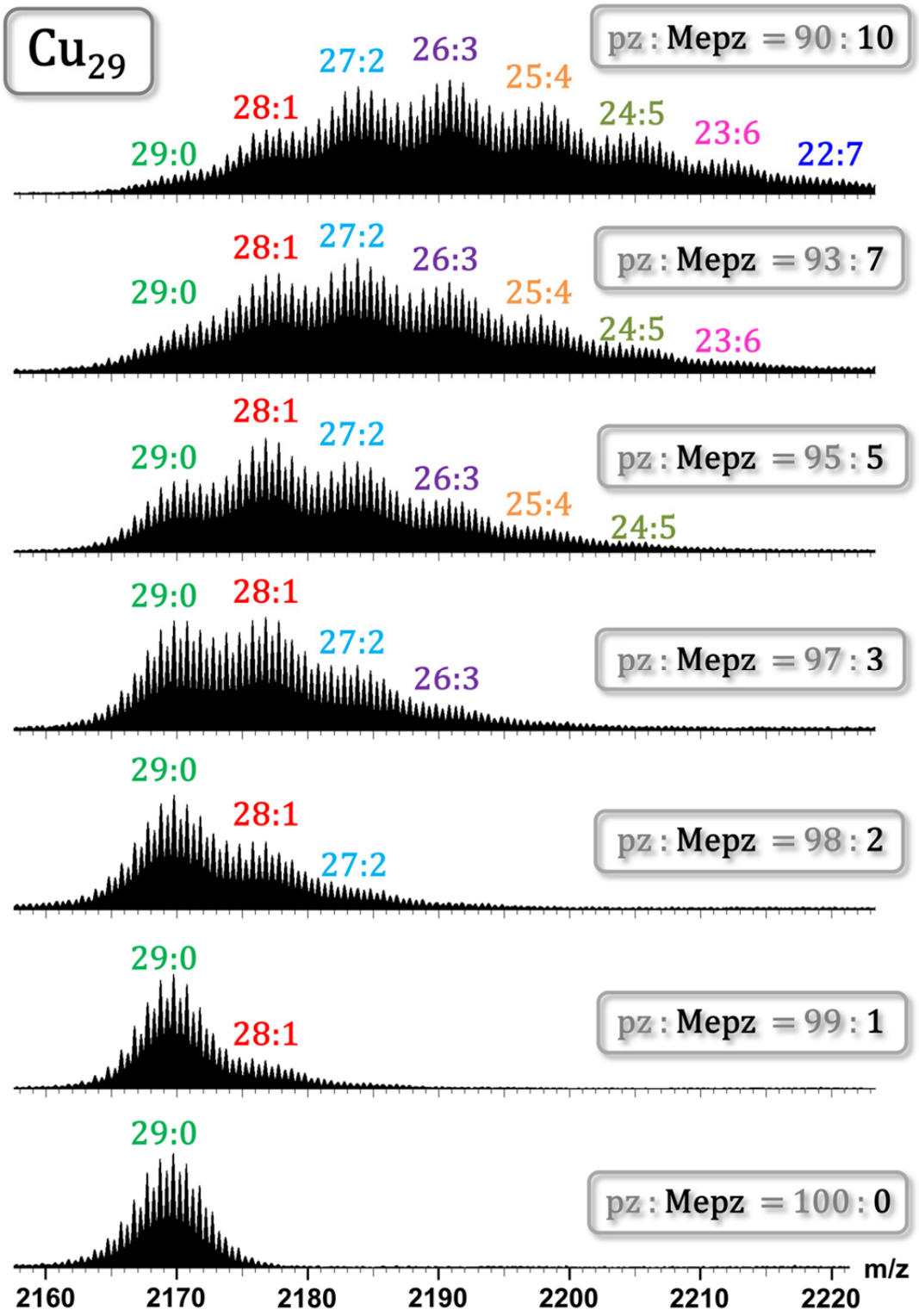

Figure S14. Zoomed portion of the ESI-MS(−) spectra of the $(Bu_4N)_2[CO_3\subset\{Cu_n(OH)_n(pz)_{n-x}(4\text{-Mepz})_x\}]$ (n = 27, 29, 30, 31) nanojar mixtures obtained using 0−10 mol% 4-MepzH..

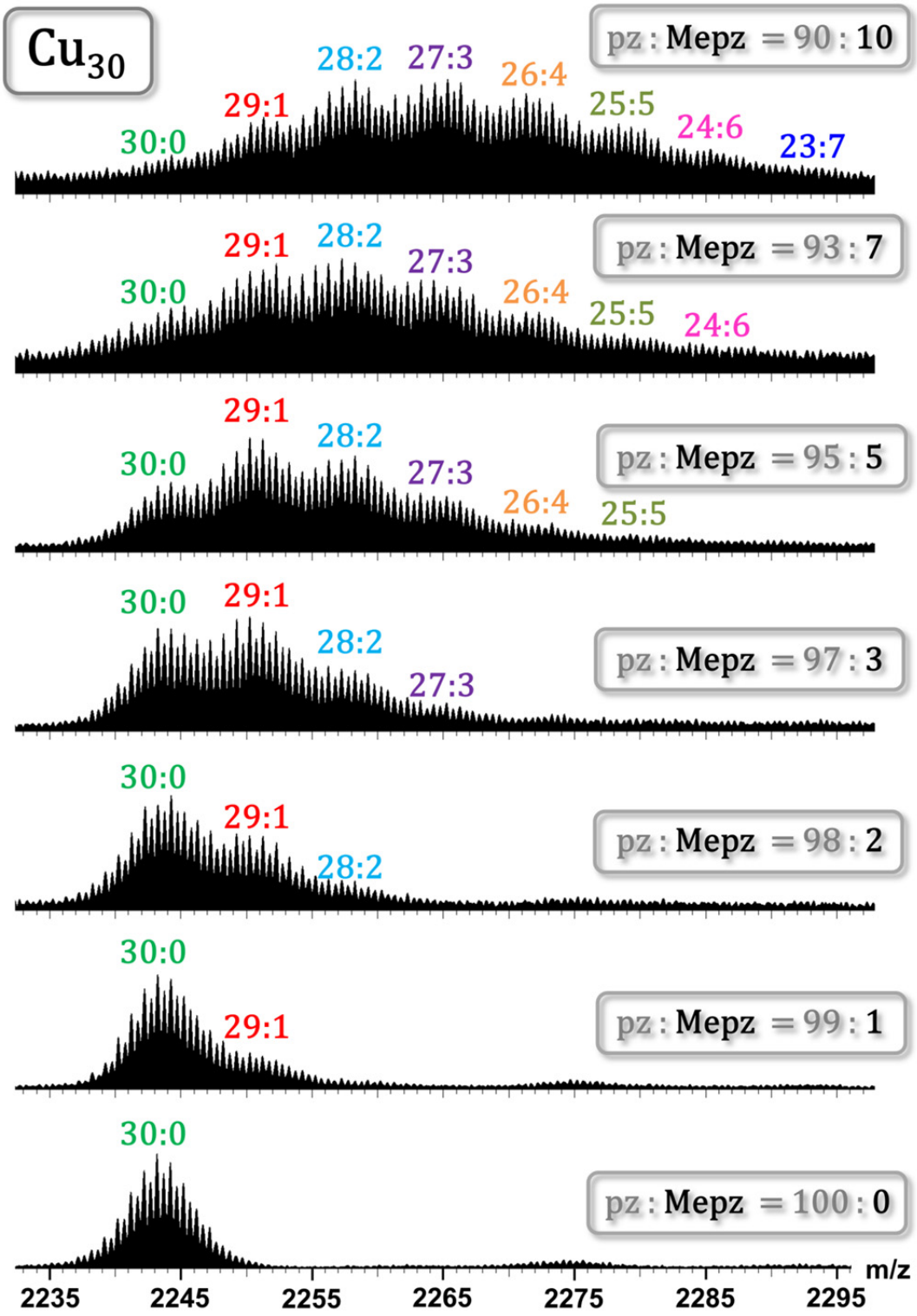

Figure S15. Zoomed portion of the ESI-MS(−) spectra of the $(Bu_4N)_2[CO_3\subset\{Cu_n(OH)_n(pz)_{n-x}(4\text{-Mepz})_x\}]$ (n = 27, 29, 30, 31) nanojar mixtures obtained using 0−10 mol% 4-MepzH..

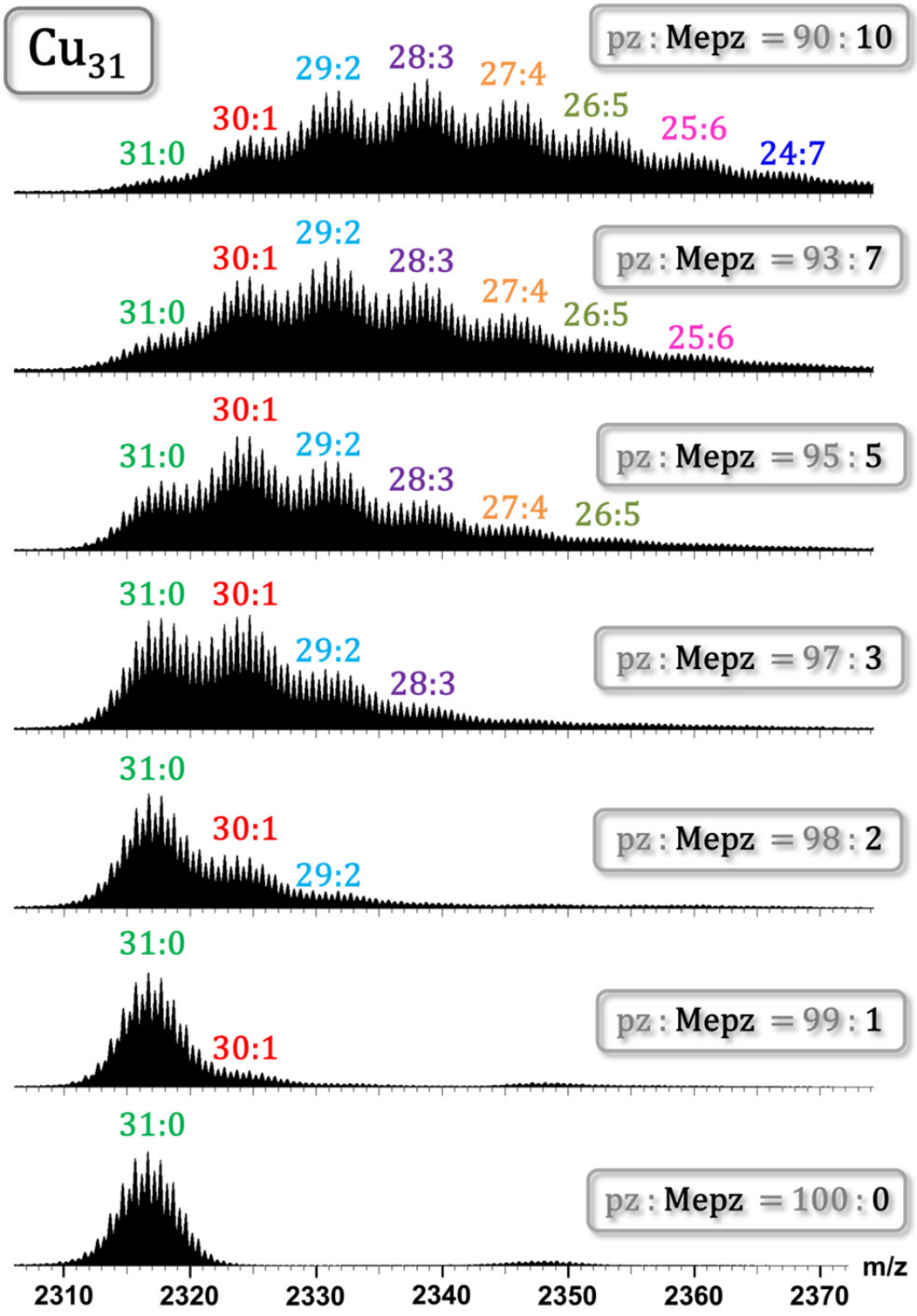

Figure S16. Zoomed portion of the ESI-MS(−) spectra of the $(Bu_4N)_2[CO_3\subset\{Cu_n(OH)_n(pz)_{n-x}(4\text{-Mepz})_x\}]$ (n = 27, 29, 30, 31) nanojar mixtures obtained using 0–10 mol% 4-MepzH.

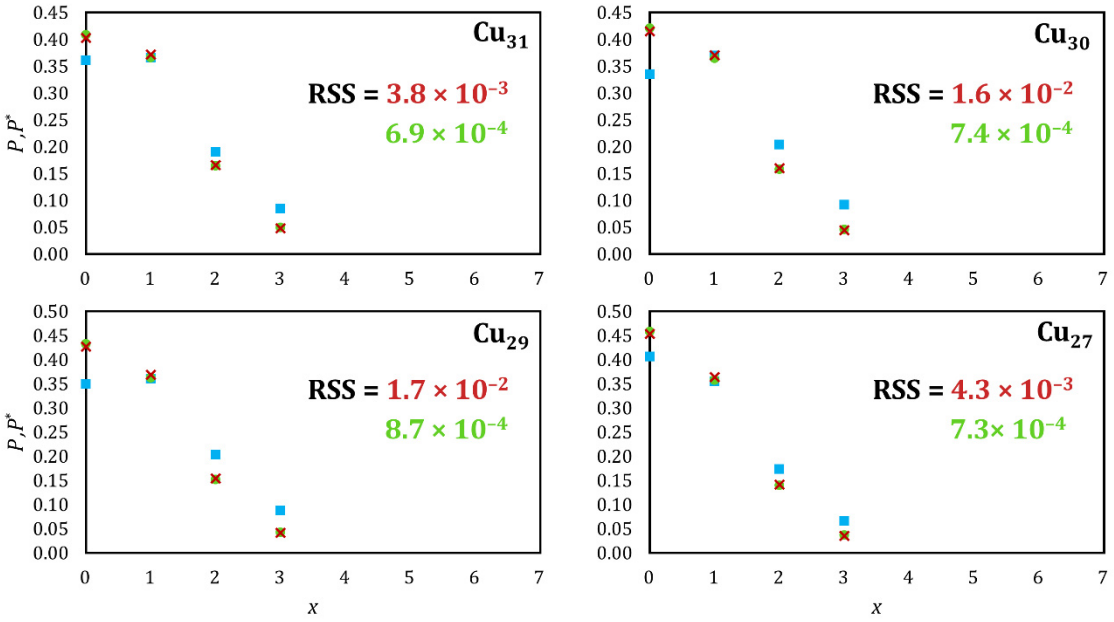

Figure S17. Plots of binomial (red), Poisson (green) and experimental (blue) distributions for different sized nanojars with 97:3 pz:4-Mepz ligand mixture.

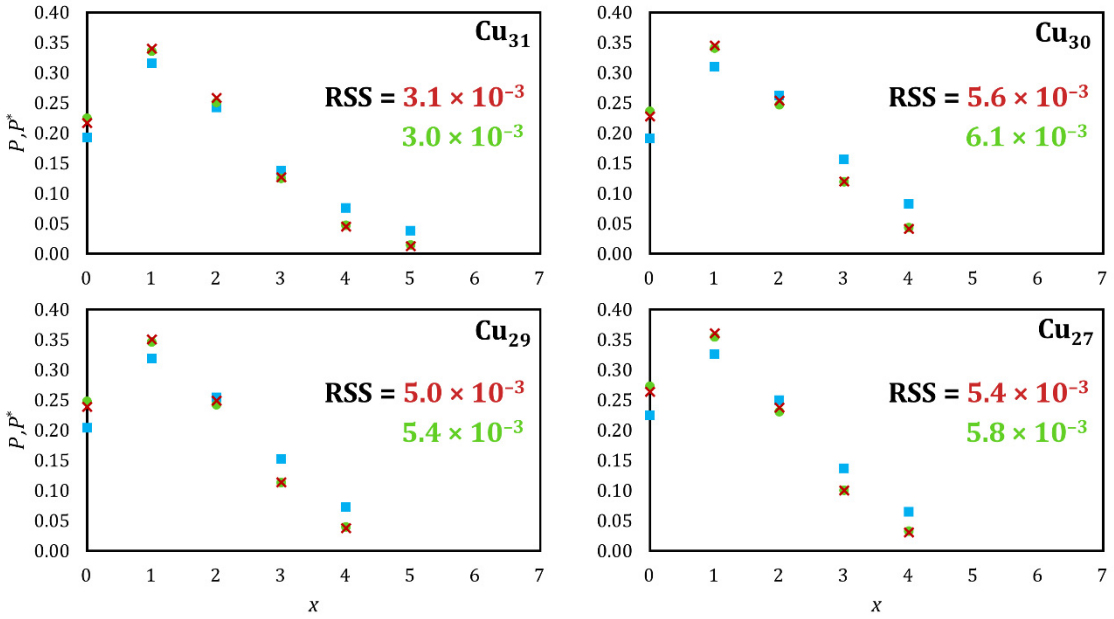

Figure S18. Plots of binomial (red), Poisson (green) and experimental (blue) distributions for different sized nanojars with 95:5 pz:4-Mepz ligand mixture.

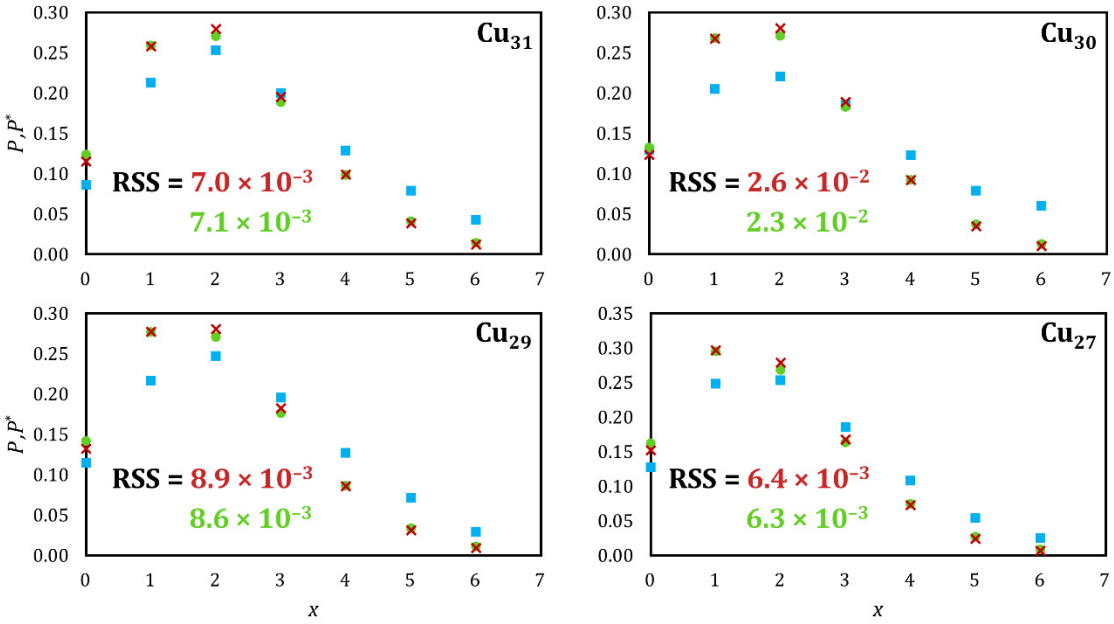

Figure S19. Plots of binomial (red), Poisson (green) and experimental (blue) distributions for different sized nanojars with 93:7 pz:4-Mepz ligand mixture.

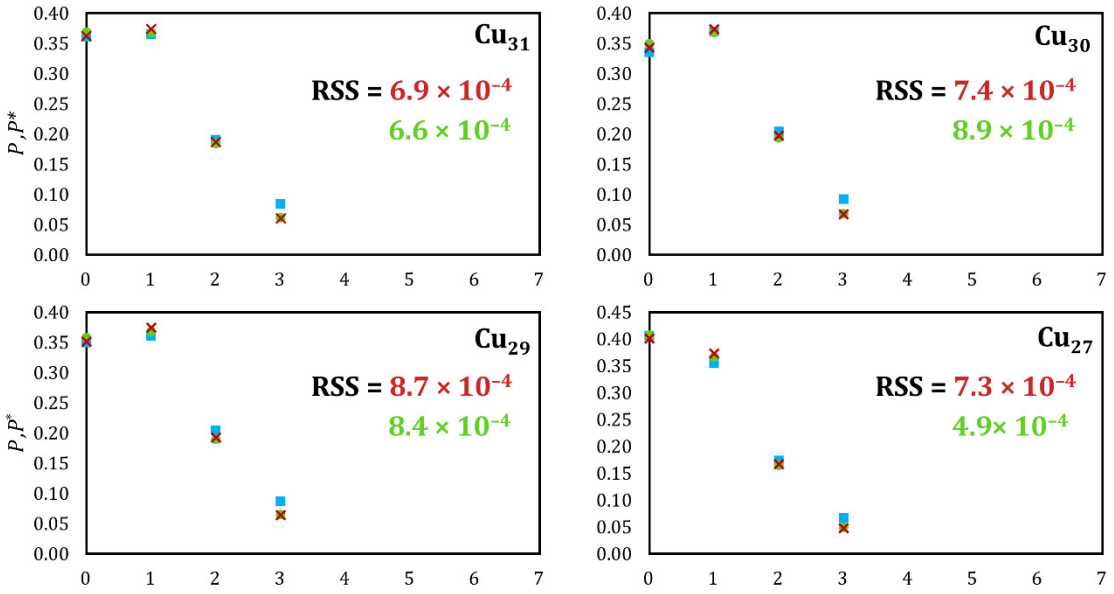

Figure S20. Plots of binomial (red), Poisson (green) and experimental (blue) distributions using j_{ad} for different sized nanojars with 97:3 pz:4-Mepz ligand mixture.

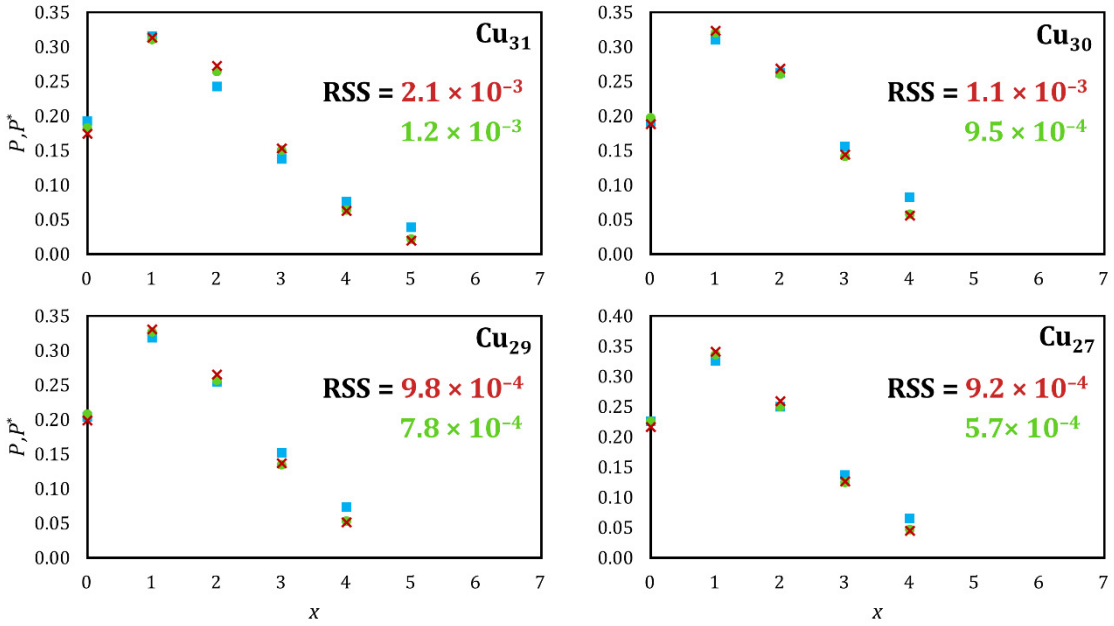

Figure S21. Plots of binomial (red), Poisson (green) and experimental (blue) distributions using j_{ad} for different sized nanojars with 95:5 pz:4-Mepz ligand mixture.

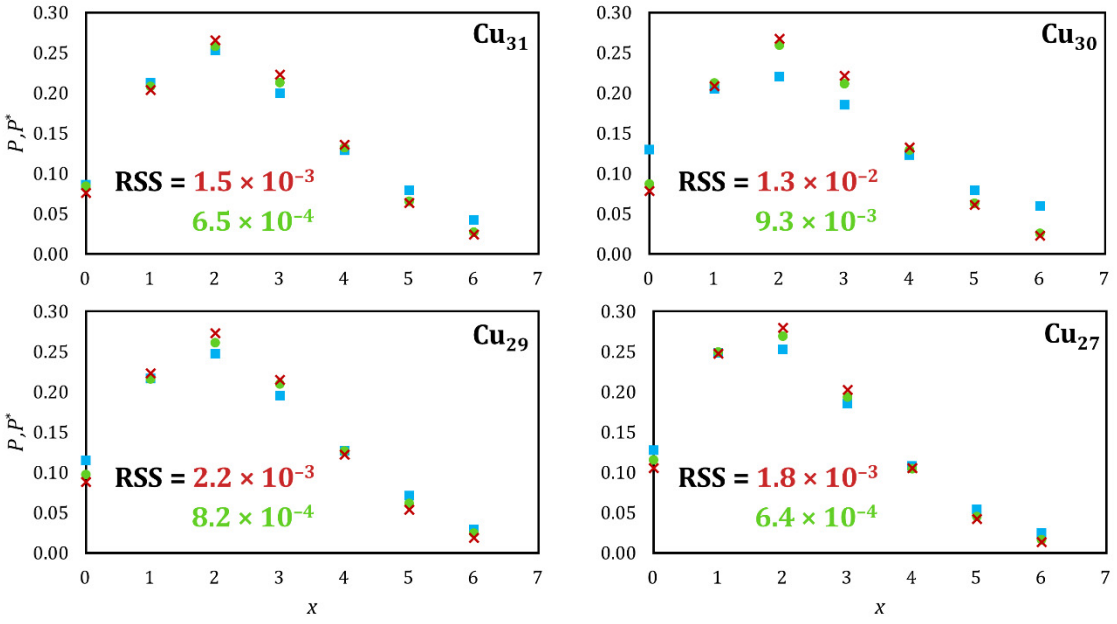

Figure S22. Plots of binomial (red), Poisson (green) and experimental (blue) distributions using j_{ad} for different sized nanojars with 93:7 pz:4-Mepz ligand mixture.